

Journal of Materials and Engineering Structures

Research Paper

Empirical vibration investigation of homogeneous ground with shallow tunnel by low-frequency excitation

Thu-Hang Tran [a,*], ***Duc-Phong Pham*** [b]

[a] *University of Transport and Communications, 3 Cau Giay street, Hanoi, Vietnam*

[b] *Le Quy Don Technical University, 236 Hoang Quoc Viet street, Hanoi, Vietnam*

ARTICLE INFO

Article history:

Received : 12 November 2024

Revised : 21 December 2024

Accepted : 24 December 2024

Keywords:

Low-frequency excitation

Shallow tunnel

Loose fine sand foundation

Shaking table

ABSTRACT

Urban tunnels and underground structures usually stay at small overburden heights. The insight of shallow underground structures' behaviours is challenging. Low-frequency seismic waves can create significant deformations to civil structures, so the prediction and warning of the damage possibility of a low-frequency earthquake to the civil infrastructure has attracted research attention. This paper presented an experimental investigation on a physical model including a homogeneous ground and a shallow tunnel. The model underwent an artificial harmony low-frequency excitation created by a 2x2m shaking table. The vibration characteristics of the model's components were studied and discussed. The accelerograms and the FFT spectrum analysis was realised to understand the similarity of the input and output signals. The Cumulative Absolute Velocity and the Arias Intensity were determined and the correlation between them was investigated. The results proved the complexity of the vibration behaviours of the physical model during the artificial earthquake. The severe effect of the low-frequency excitation on the ground and underground structure motion was also detected.

1 Introduction

As an alternative living space for the ground, especially in urban areas, the underground has been exploited early in history. The underground utilisation, however, is always challenging. Among the difficulties, the vibration behaviours of the underground structures and the foundations are complicated. When an external excitation was created and applied in the ground, the vibration propagation insight was challenged because it is affected by many factors, such as the properties of the ground and excitation [1]. The most popular vibration sources for the ground vibration propagation study were artificial, such as blasting, pile driving, ultrasonic, rail and road traffic [2]. Earthquakes are a particular type of ground excitation. It is a natural hazardous excitation that appears from the epicentre, deeply stays in the ground, transfers the seismic wave to the ground surface, and liberates the seismic energy. Under seismic application, deep-buried structures

* *Corresponding author. Tel.: +84915085660.*
E-mail address: tranthuhang@utc.edu.vn

e-ISSN: 2170-127X, (cc) BY-SA

RESEARCH REVIEW of Sciences and Technologies

usually exhibit better vibration behaviours than shallow-buried ones [3]. While many parts of the urban underground infrastructures stay near the ground surface, the insight of shallow underground structures' behaviours is challenging. The experimental studies are executed on large or small-scale models having specific similarities with the prototypes [4]. When they undergo the excitation made by the artificial vibration waves (generally in the form of acceleration or velocity versus time curves), their responses are collected, and their mechanical behaviours are analysed. The shaking table and the centrifuge testing are currently two experimental seismic solutions [5]. Besides the measured in-situ data from the ground monitoring and the numerical results from the theoretical and mathematical calculations, the obtained output from the empirical campaigns provides comprehensive information on the mechanical and vibration nature of the investigated object.

The seismic high-frequency ground motions ($f_{dominant}$> 10Hz) propagate more quickly but release more quickly the seismic energy than the low-frequency ones ($1 \leq f_{dominant} \leq 10$). Low-frequency seismic waves tend to create more significant displacements and faster vibration velocity increments. The need for low-frequency studies in seismology has been proven [6]. The prediction and warning of how damage a low-frequency earthquake can cause to the civil infrastructure has attracted research attention. A sensitive but conservative parameter that can be used as a threshold for warning the seismic potential damage has been in search. Although the Peak Ground Acceleration (PGA, m/s^2) is the most popular physical quantity that displays the seismic severity since the acceleration signals can be measured during an earthquake, it is not sensitive and comprehensive enough. The Cumulative Absolute Velocities (CAV, m/s) appeared in the Report NP5930 of the American Electric Power Research Institute (EPRI) in 1988 to express how fast a vibration changes during the excitation process [7]. In the Operating Basis Earthquake (OBE), a criterion for the shut-down requirement of nuclear facilities during an earthquake, the checking is required for the response spectrum and the CAV, successively. In an analysis of the OBE Exceedance Working Panel of EPRI on 263 ground motions caused by earthquakes, the CAV was the best parameter for identifying the potential seismic damage compared to five parameters [8]. The parameter is a robust ground motion parameter since it integrates the motion's amplitude, the frequency and the duration [9]. The CAV is more sensitive to low-frequency motions than high-frequency ones and strongly correlates with seismic intensity [7]. The CAV has been applied to nuclear power plants [8], civil structures, and urban areas, with the application of earthquake early warning systems [10]. The value of CAV = 0.3g (m/s) (with g: gravity acceleration, m/s^2) was proposed as the threshold for the strong ground motions of intensity VI earthquakes in the Modified Mercalli Intensity scale (MMI VI) [8]. Under this limit, the seismic activity is considered slight and causes no significant damage to building structures [11]. The Arias Intensity (AI, m/s) is a parameter that indicates the strength of the ground motion. While CAV is the time integral of the ground acceleration during the seismic, AI is the time integral of the square of the ground acceleration. It shows the cumulative energy dissipation during the excitation process, which is used as a seismic energy and damage potential indicator [12]. CAV and AI are robust seismic parameters since they consider the acceleration amplitude, the motion duration, and the frequency. The correlativity between them was found to be significant [13, 14]. The threshold value AI = 0.07g (m/s), equivalent to the threshold value CAV = 0.3g (m/s), was chosen by Reed and Kassawara [8].

Under this light, a study of low-frequency vibration propagation in a homogeneous ground, including a shallow buried structure, was done using physical modelisation. The rigid box soil container was chosen and created to embrace a circular small-scale tunnel model. The loose fine black sand, typically found in the Red River delta (Northen of Vietnam), was the filling soil. An artificial low-frequency ground motion was created on the shaking table with an input harmony sinusoidal accelerogram. The acceleration of the soil container and the tunnel model were measured and studied. The vibration propagation in the physical model was investigated using the subtraction of two obtained acceleration data sets. On the obtained data, the configurations of the motion curves were compared, and the dominant frequencies were determined by the Fast Fourier Transform (FFT) spectrum analysis. The energy and possibility of damage caused by the vibrations were investigated through CAV and AI's absolute values and tendencies. In this paper, after describing the experiment establishment, the results and discussions were presented, and the conclusions were proposed.

2 Experiment establishment

The diameter of the tunnel model was D = 0.30m. The rigid box container was made with a steel frame and hard transparent polycarbonate plates. The small-scale tunnel model stayed in the middle of the container, and the surrounding areas were filled with the Red River loose fine black sand. The total physical model included the soil container, the tunnel model and the filling soil. It was mounted on the 2x2m shaking table. Two acceleration gauges were attached at the same

height at the container's wall and the tunnel model. The configuration of the physical model for the table shaking testing is presented in Figure 1.

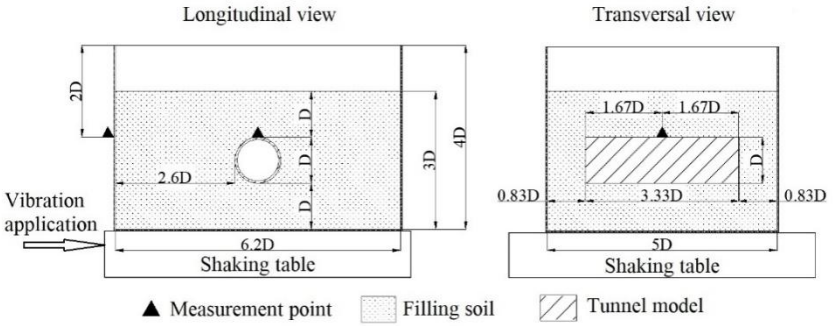


Fig. 1 – Configuration of the physical model mounted on the shaking table

An artificial harmonic sinusoidal accelerogram was used as the input data to operate the shaking table. It was composed of three segments with the same dominant frequency. It created the vibration along the longitudinal view of the physical model. The principal parameters of the input accelerogram are presented in Table 1.

Table 1 – Parameters of the input accelerogram

Segment	Dominant frequency (Hz)	Peak Ground Acceleration (PGA, m/s^2)	Time interval (s)	Duration (s)
1st	3.479	0.029	(0 ; 6.570)	6.570
2nd	3.479	0.290	(6.570 ; 36.570)	30.000
3rd	3.479	0.029	(36.570 ; 45.000)	8.430

Once the shaking table had been operated with the input data, a uni-directional vibration was created and transferred from the shaking table to the physical model's components. The accelerations measured in two gauges were studied, and the model's vibration was investigated. In this paper, the input data was named the "Shaking table". The acceleration measured at the gauges on the container's wall was named the "Soil container", and the one measured at the gauges on the tunnel model was named the "Tunnel model". A vibration obtained by subtracting the Soil container and Tunnel model's data was named the "Filling soil". The vibration characteristics of all vibrations were also named in the same manner. Examining and discussing their differences helped to understand the vibration propagation in the experimental campaign.

3 Experiment results and discussions

3.1 Acceleration versus time relationship

The acceleration versus time relationship between the vibrations of the shaking table and the physical model during the experiment was built. The accelerograms were sketched and are presented in Figure 2.

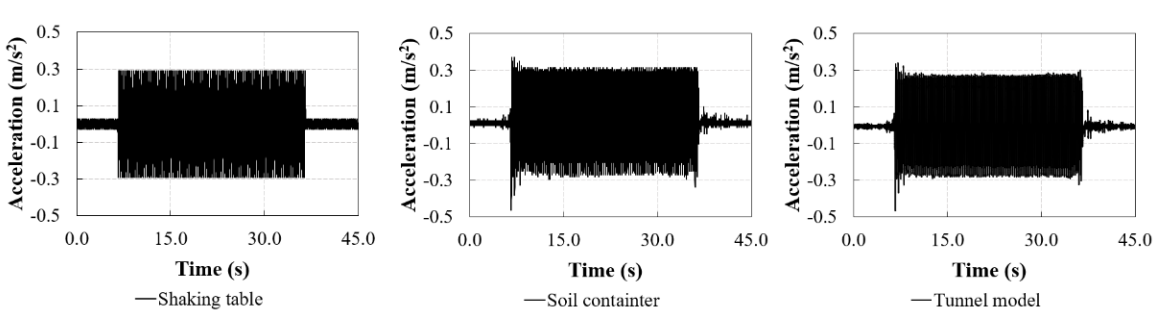


Fig. 2 – Accelerograms of Shaking table, Soil container and Tunnel model

All vibrations could be divided into three time intervals: (a) 1st segment: t = (0.000 ; 6.570) (s); (b) 2nd segment: t = (6.570 ; 36.570) (s); (c) 3rd segment: t = (36.570 ; 45.000) (s). Examining the geometrical appearance of the accelerograms exhibited the geometrical differences between them. The results are presented in Table 2.

Table 2 - Geometrical characteristics of the accelerograms

Segment	Accelerogram	Form	PGA (m/s^2)
1st and 3rd	Shaking table	Theoretical harmonic	0.029
	Soil container	Quasi-straight line	0.023
	Tunnel model	Quasi-straight line	-0.005
2nd	Shaking table	Theoretical harmonic	0.290
	Soil container	Quasi-harmonic	0.315
	Tunnel model	Quasi-harmonic	0.285

Three accelerograms were horizontally symmetrical, and their overall geometrical appearance was similar. There were some divergences between the two measured vibrations and the input vibration. However, no abnormal output signals were captured. The stability of the physical during the experiment was confirmed. For better observation of the differences between the three accelerograms, three time segments of the accelerograms were captured as the representatives of three vibration segments (see Figure 3).

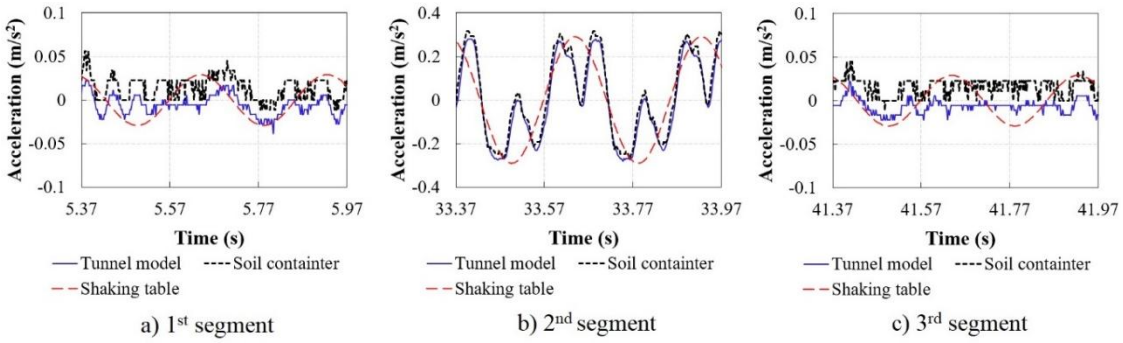


Fig. 3 – Comparison of the accelerograms in three time segments

The shape dissimilarity of the accelerograms in the 1st and 3rd vibration segments was considered as the consequence of the minor input wave (PGA < 0.003g) and the accuracy of the shaking table's control. The geometrical analysis was insufficient to conclude the conformity between these vibrations.

In this study, the hypothesis of which the subtraction of the Soil container and Tunnel model's data was the Filling soil's vibration was taken. This meant that a part of the vibration wave propagated from the Soil container was kept by the Filling soil, and the rest was transferred into the Tunnel model. The vibration propagation understanding was gained by comparing the vibration of three physical model components. The Filling soil's accelerogram was built, and its configuration was examined (see Figure 4 and Table 3).

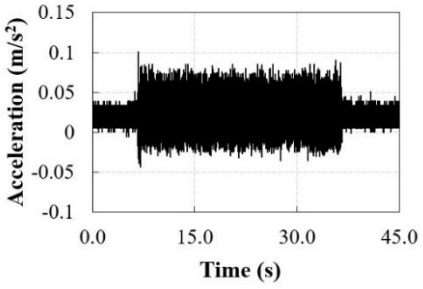


Fig. 4 – Filling soil's accelerogram

Table 3 – Geometrical characteristics of Filling soil's accelerogram

Segment	Form	PGA (m/s^2)
1st and 3rd	Quasi-straight line	0.028
2nd	Quasi-harmonic	-0.031

The overall structure of this accelerogram was similar to the three previous ones. However, this curve was not horizontally symmetrical and showed a movement to the first quadrant of the graph. The three model's components took the same geometrical type. The similarity between Soil container and Tunnel model proved the smooth vibration propagation in the physical model. The gradual diminution of the vibration data from Soil container to Tunnel model to Filling soil was understood as the protection effect of Filling soil to Tunnel model. Further study on the vibration characteristics was needed to clarify the similarity between the four vibrations. The details are presented in the next parts of this paper.

3.2 Spectrum analysis

The Fast Fourier Transform (FFT) spectrum analysis was conducted to verify whether the vibration waves had the same principal characteristics. The dominant frequency and corresponding amplitude of each vibration were found. The results are presented in Table 4 and Figure 5.

Table 4 – FFT spectrum analysis results

Parameter	Unit	Shaking table	Soil container	Tunnel model	Filling soil
Dominant frequency	Hz	3.479	3.479	3.479	3.479
Amplitude (acceleration)	m/s^2	0.273	0.189	0.188	0.005
Frequency curve shape		Single peak	Multi-peak	Multi-peak	Multi-peak

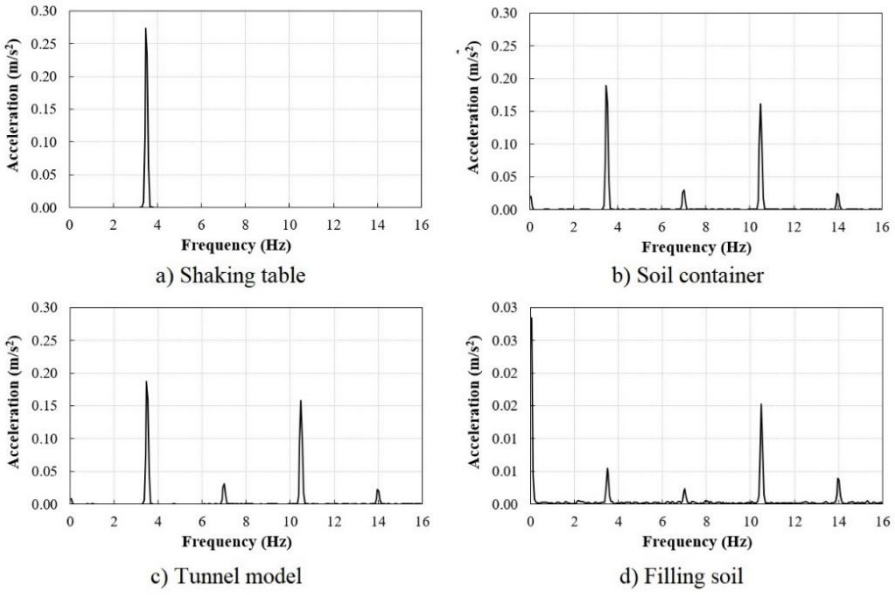


Fig. 5 – Acceleration versus frequency graphs by FFT spectrum analysis

The overall configuration of all the acceleration versus frequency graphs was reasonable. The larger the amplitudes in the accelerograms, the higher the amplitudes in the FFT spectrums. The results from Table 4 and Figure 5 exhibited the differences between the input wave (Shaking table) and the output waves (Soil container, Tunnel model and Filling soil). While there was one single peak on the first graph, several multiplications of the base peak were found on the three remaining graphs. However, those multi-peaks were ignored, and the dominant frequency values of all vibrations were identical ($f_{dominant}$ = 3.479Hz). The presence of the undertone and overtone in the vibration of the physical model's components could be attributed to the bias in the computer control of the shaking table. It was considered as the

explanation for the dissimilarity between the input and measured accelerograms. Through the spectrum analysis of the accelerograms by FFT function, the dominant frequencies, their amplitudes, and the structure of the frequency graphs were found for all vibrations. A reasonable correspondence between the vibration waves and their FFT spectrum was obtained. The appearance of the undertone and overtone on the frequency spectrum of the physical model was neglected. The divergence between the input and output data was attributed to the accuracy of the table control.

3.3 Cumulative absolute velocity

The Cumulative Absolute Velocity (CAV, m/s) was calculated with the following equation

$$\mathrm{CAV} = \int_{t=0}^{45} |a(t)| dt = \sum_{t=0}^{45} \frac{\left(\left|a_{t_i} + a_{t_{i+1}}\right|\right)}{2} \times (t_{i+1} - t_i) \quad (1)$$

In this equation, a(t) was the acceleration versus time function (m/s^2), a_{ti} (m/s^2) was the acceleration value at time t_i (s), a_{ti+1} (m/s^2) was the acceleration value at time t_{i+1} (s), and t (s) was the excitation duration t = (0 ; 45) (s).

The CAV vs time curves of four vibrations are presented in Figure 6.

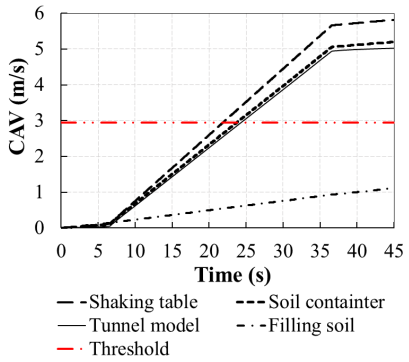


Fig. 6 – CAV versus time curves of vibrations

The threshold value CAV = 0.3g = 2.943m/s was examined. Three vibrations of the Shaking table, Soil container, and Tunnel model reached the threshold at the time t = 21.828s, 23.702s, and 24.298s, respectively. The time interval Δt_1 = 1.874s when the Shaking table and Soil container reached the threshold was considered the machine control time lag. The time interval Δt_2 = 0.596s between the Soil container and Tunnel model was attributed to the presence of the Filling soil that delayed the threshold touching of the Tunnel model. The Filling soil did not surpass the CAV threshold.

The theoretical CAV versus time functions of all vibrations were searched to learn the variation tendency of the obtained CAV versus time curves. The CAV versus time functions and their accurate ratio, represented by the R-square values, were listed in Table 5.

Table 5 – Theoretical function of CAV versus time curves and its R-square value

Vibration	1st segment	2nd segment	3rd segment
Shaking table	y = 0.018x (R^2 = 1.000)	y = 0.185x - 1.092 (R^2 = 1.000)	y = 0.018x + 4.987 (R^2 = 1.000)
Soil container	y = 0.016x (R^2 = 0.999)	y = 0.164x - 0.958 (R^2 = 1.000)	y = 0.017x + 4.445 (R^2 = 0.999)
Tunnel model	y = 0.007x-0.001 (R^2 = 0.986)	y = 0.162x - 1.005 (R^2 = 1.000)	y = 0.009x + 4.618 (R^2 = 0.977)
Filling soil	y = 0.026x - 0.015 (R^2 = 0.999)	y = 0.026x - 0.015 (R^2 = 0.999)	y = 0.026x - 0.015 (R^2 = 0.999)

The structure of the CAV versus time curves of the Shaking table, Soil container and Tunnel model were in the same form of a three-segmental line. The development rule of the Soil container and Tunnel mode adapted well to the one of the Shaking table. The 1st and 3rd segments of all CAV versus time curves were nearly horizontal, which meant the quasi-null velocity variation during these periods. Whereas the 2nd segments of the three first CAV versus time curves had steeper slopes, it showed the faster monotonic increase tendency of all the vibrations. The slopes of the CAV versus time curves reduced gradually from the Shaking table's curve (0.185) to the Soil container's (0.164) and the Tunnel model's (0.162). Besides, the Filling soil's curve is a single segmental line in all vibration periods. It was understood that when the excitation started and the vibration propagated in the Filling soil, the ground's vibration velocity increased continuously regardless of the vibration source. The CAV variation investigation exhibited the damage potential threshold equivalent to MMI VI, and the CAV threshold exceedance occurrences were found in the vibration of the Shaking table, Soil container and Tunnel model. It was understood that the artificial earthquake created by the shaking table had the possibility of making significant damage to the tunnel [8]. This fact proved the low-frequency excitation's severe effects on the ground and underground structure motions. The fast velocity variation, presented by the steep slope of CAV-time curves, was blamed for the phenomenon.

3.4 Arias Intensity

The Arias Intensity (AI, m/s) was calculated with the following equation

$$\mathrm{AI} = \frac{\pi}{2g}\int_{t=0}^{45}[a(t)]^2 dt \tag{2}$$

In this equation, a(t) was the acceleration versus time function (m/s^2), t (s) was the excitation duration t = (0 ; 45) (s), and g was the gravity acceleration (m/s^2).

The AI versus time curves of four vibrations are presented in Figure 7.

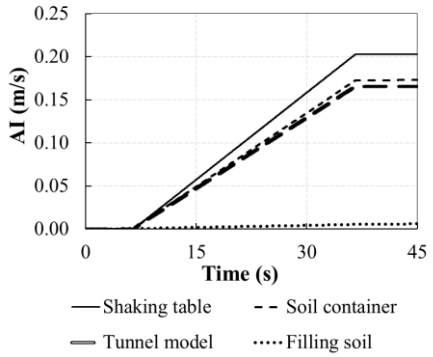


Fig. 7 – AI versus time curves of vibrations

The threshold value AI = 0.07g = 0.687m/s was examined. None of the vibrations reached the AI threshold. The tendencies of the AI versus time curves were searched, and the results are shown in Table 6.

Table 6 – Theoretical function of AI versus time curves and its R-square value

Vibration	1st segment	2nd segment	3rd segment
Shaking table	y = 0.000 (R^2 = 0.999)	y = 0.007x - 0.003 (R^2 = 1.000)	y = 0.000x + 0.200 (R^2 = 0.999)
Soil container	y = 0.000 (R^2 = 0.982)	y = 0.006x - 0.036 (R^2 = 1.000)	y = 0.000x + 0.170 (R^2 = 0.995)
Tunnel model	y = 0.000 (R^2 = 0.549)	y = 0.005x - 0.034 (R^2 = 1.000)	y = 0.000x + 0.165 (R^2 = 0.960)
Filling soil	y = 0.0001x - 0.0003 (R^2 = 0.996)	y = 0.0001x - 0.0003 (R^2 = 0.996)	y = 0.0001x - 0.0003 (R^2 = 0.996)

The AI versus time curves of the Shaking table, Soil container and Tunnel model were three-segmental lines. The Soil container and Tunnel model's variation tendency was similar to the Shaking table's. The 1st and 3rd segments of the three mentioned curves were almost parallel with the horizontal axe, which meant the quasi-zero AI modification during these periods. The 2nd segment of the three mentioned curves was mono-inclined, and the segment's slopes showed the AI's augmentation speed during the excitation time. The curve's slopes decreased from the case of the Shaking table (0.007) to the Soil container (0.006) and the Tunnel model (0.005). Meanwhile, the Filling soil's curve was a mono-inclined line, and its slope was considerably small (0.001).

The AI-time curves and the CAV-time curves were compared. Their geometrical appearances were similar, which confirmed the strong correlation between them concluded by Bradley [13] and Poreddy [14]. Two parameters were almost frozen during the excitation's starting and closing period. In the excitation's main period, the AI and CAV developed quickly, but the speed decreased from the Shaking table to the Soil container to the Tunnel model. For the case of the Filling soil, two parameters were augmented gradually during the experiment. It showed the progressive energy accumulation caused by the artificial earthquake during the vibration propagated in Filling soil. The threshold value of AI and CAV were examined but only the latter appeared. It could be understood as the higher sensitivity of CAV to AI in warning of the seismic damage possibility of the low-frequency ground motions. It proved the recommendations of the EPRI's OBE Exceedance Working Panel [8]. It also demonstrated Brendon's remark on the differences between the two parameters and the better suitability of AI for high-frequency ground motions [13].

4 Conclusions

An empirical vibration investigation of a physical model, including a small-scale tunnel model, the surrounding ground by Red River loose fine black sand, and a rigid box soil container, had been established. The model underwent a harmony sinusoidal low-frequency wave excitation created by the shaking table in the laboratory of the University of Transport and Communications (on the Hanoi campus, Vietnam). During the artificial earthquake, the vibration of the physical model was measured, and the data processing was done to understand the model's vibration nature. The stability of the physical model on the shaking table during the testing was confirmed by the normal behaviours of the physical model and the tendency similarity of the vibration characteristics during the testing. The experiment showed the obvious effect of the low-frequency ground motions on the ground and the underground structure. Small PGA seismic waves could bring hazardous actions because of the high-velocity variation of the vibration in short time durations. The complexity of the ground vibration behaviour was proven when the ground's CAV and AI increased continuously regardless of the vibration source. While the correlation between CAV and AI was confirmed, the higher sensitivity of CAV to AI in warning of the seismic damage possibility of the low-frequency ground motions was demonstrated.

Acknowledgements

Great appreciation was given to the University of Transport and Communications (Vietnam) for supporting the research.

REFERENCES

[1]- D.-S. Kim, J.-S. Lee, Propagation and attenuation characteristics of various ground vibrations. Soil Dynamics and Earthquake Engineering, 19(2) (2000) 115-126. doi:10.1016/S0267-7261(00)00002-6.

[2]- T.G. Gutowski, C.L. Dym, Propagation of ground vibration: A review. Journal of Sound and Vibration, 49(2) (1976) 179-193. doi:10.1016/0022-460X(76)90495-8.

[3]- Y.M.A. Hashash, J.J. Hook, B. Schmidt, J. I-Chiang Yao, Seismic design and analysis of underground structures. Tunnelling and Underground Space Technology, 16(4) (2001) 247-293. doi:10.1016/S0886-7798(01)00051-7.

[4]- M.A. Meguid, O. Saada, M.A. Nunes, J. Mattar, Physical modeling of tunnels in soft ground: A review. Tunnelling and Underground Space Technology, 23(2) (2008) 185-198. doi:10.1016/j.tust.2007.02.003.

[5]- G. Tsinidis, F. de Silva, I. Anastasopoulos, E. Bilotta, A. Bobet, Y.M.A. Hashash, C. He, G. Kampas, J. Knappett, G. Madabhushi, N. Nikitas, K. Pitilakis, F. Silvestri, G. Viggiani, R. Fuentes, Seismic behaviour of tunnels: From experiments to analysis. Tunnelling and Underground Space Technology, 99 (2020) 103334. doi:10.1016/j.tust.2020.103334.

[6]- F.t. Kroode, S. Bergler, C. Corsten, J.W.d. Maag, F. Strijbos, H. Tijhof, Broadband seismic data — The importance of low frequencies. GEOPHYSICS, 78(2) (2013) WA3-WA14. doi:10.1190/geo2012-0294.1.

[7]- J.W. Reed, N. Anderson, N.C. Chokshi, R.P. Kennedy, W.J. Metevia, D.K. Ostrom, J.D. Stevenson, A criterion for determining exceedance of the operating basis earthquake: Final report, United States. (1988). 321.

[8]- J.W. Reed, R.P. Kassawara, A criterion for determining exceedance of the operating basis earthquake. Nuclear Engineering and Design, 123(2) (1990) 387-396. doi:10.1016/0029-5493(90)90259-Z.

[9]- S.L. Kramer, Geotechnical earthquake engineering. Prentice Hall Inc., Upper Saddle River 1996.

[10]- Y.M. Fahjan, H. Alcik, A. Sari, Applications of cumulative absolute velocity to urban earthquake early warning systems. Journal of Seismology, 15(2) (2011) 355-373. doi:10.1007/s10950-011-9229-8.

[11]- H.O. Wood, F. Neumann, Modified Mercalli intensity scale of 1931. Bulletin of the Seismological Society of America, 21(4) (1931) 277-283. doi:10.1785/bssa0210040277.

[12]- A. Arias, A measure of earthquake intensity. Seismic Design for Nuclear Plants, (1970) 438-483.

[13]- B.A. Bradley, Correlation of Arias intensity with amplitude, duration and cumulative intensity measures. Soil Dynamics and Earthquake Engineering, 78 (2015) 89-98. doi:10.1016/j.soildyn.2015.07.009.

[14]- L.R. Poreddy, M.K. Pathapadu, C. Navyatha, J. Vemuri, R. Chenna, Correlation analysis between ground motion parameters and seismic damage of buildings for near-field ground motions. Natural Hazards Research, 2(3) (2022) 202-209. doi:10.1016/j.nhres.2022.08.002.